Palaeontology The Palaeontological Association www.palass.org

[Palaeontology, Vol. 68, Part 4, 2025, e70019]

Standing giants: a digital biomechanical model for bipedal postures in sauropod dinosaurs

by JULIAN C. G. SILVA JUNIOR[1,2]*, GABRIEL S. FERREIRA[2,3], AGUSTÍN G. MARTINELLI[4], THIAGO S. MARINHO[5,6] *and* FELIPE C. MONTEFELTRO[1]

[1]Laboratório de Paleontologia e Evolução de Ilha Solteira, UNESP, Ilha Solteira, Brazil; juliancristiangoncalves@gmail.com, fc.montefeltro@unesp.br
[2]Senckenberg Centre for Human Evolution and Palaeoenvironment at the University of Tübingen, Tubingen, Germany; gabriel.ferreira@senckenberg.de
[3]Geosciences Department, Eberhard Karls Universität Tübingen, Tubingen, Germany
[4]Seccion Paleontología de Vertebrados, Museo Argentino de Ciencias Naturales 'Bernardino Rivadavia'-CONICET, Buenos Aires, Argentina; agustin_martinelli@yahoo.com.ar
[5]Centro de Pesquisas Paleontologicas L. I. Price, Complexo Cultural e Científico Peirópolis, Pró-Reitoria de Extensão Universitária, Universidade Federal do Triângulo Mineiro, Uberaba, Brazil; thiago.marinho@uftm.edu.br
[6]Departamento de Ciências Biológicas, Instituto de Ciências Exatas, Naturais e Educação, Universidade Federal do Triângulo Mineiro, Uberaba, Brazil
*Corresponding author

Typescript received 28 October 2024; accepted in revised form 12 June 2025

ABSTRACT: Here we explore the potential of sauropod dinosaurs to adopt a bipedal or tripodal stance using digital biomechanical modelling and finite element analysis (FEA). Seven sauropod species from diverse lineages and sizes were sampled, and 3D models of their femora were analysed under both extrinsic (body weight distribution) and intrinsic (muscular force) functional scenarios. The results indicate that smaller sauropods, like the saltasaurid titanosaur *Neuquensaurus*, were more capable of sustaining bipedal postures, probably due to their robust femora combined with advantageous muscle attachment areas. In contrast, larger sauropods such as *Dreadnoughtus* experienced higher stress levels, making bipedal postures less likely for extended periods. Our analysis provides new insights into sauropod functional evolution, highlighting that species size and morphology significantly influenced their ability to rear up, which could have played a role in behaviours such as feeding, defence and reproduction.

Key words: standing postures, functional morphology, finite element analysis, Sauropoda.

SAUROPODS are iconic dinosaurs easily recognized by their elongated necks and tails, small heads, massive and columnar limbs, and especially the colossal size they could reach, making them the largest herbivores of all times (Dodson 1990; Upchurch *et al.* 2004; Carballido *et al.* 2017; Paul 2019). In recent years, considerable attention has been paid to the palaeobiological aspects of their lives, aiming to understand how gigantism influenced their physiology, feeding strategies, and locomotion (e.g. Sander *et al.* 2011; Taylor *et al.* 2011; Otero & Hutchinson 2022).

A long-standing question directly related to their massive size is whether these animals could rear up, assuming what Bakker (1986) called a 'tripodal stance', in which the animal stands on its hindlimbs using its tail for additional support. It has been suggested that this behaviour facilitated high-browsing feeding (Hatcher 1901; Mallison 2011) or was a means for copulation and defence (Borsuk-Białynicka 1977; Bakker 1978; Alexander 1985).

In recent years, virtual palaeontology has become increasingly relevant to uncover new aspects of ancient life (Cunningham *et al.* 2014; Rowe & Rayfield 2022) and has also been applied to better understand sauropod palaeobiology (e.g. Klinkhamer *et al.* 2018; Jannel *et al.* 2019; Vidal *et al.* 2020, Lefebvre *et al.* 2022). One important technique in virtual palaeontology is finite element analysis (FEA), which is capable of simulating stress, strain, and deformation in various structures in the virtual environment (Rayfield 2007). Specifically for sauropods, this methodology has produced valuable results in areas such as feeding habits (Young *et al.* 2012), mass estimates (Falkingham *et al.* 2010), the assessment of defensive structures (Silva Junior *et al.* 2019), and the reconstruction of soft tissue structures related to mobility (Jannel *et al.* 2022).

Here, we modelled sauropod femora and applied FEA to simulate the stress that these structures could endure during a putative bipedal stance and test the hypothesis that these gigantic animals could exhibit such behaviour. We modelled two different functional cases: an extrinsic scenario, in which we applied external mass loads to simulate the animal on its hindlimbs only; and an

doi: 10.1111/pala.70019

intrinsic scenario, in which we calculated the muscle-driven stress involved in rearing movement.

MATERIAL & METHOD

Taxon sampling

Seven sauropod femora were selected for virtual modelling, aimed at sampling for as broad as possible range of different lineages (Fig. 1), sizes, and peculiar anatomical characteristics putatively related to the rearing up (see Discussion). The first sampled group, Flagellicaudata, includes the lineages Diplodocidae and Dicraeosauridae (Whitlock 2011). Diplodocidae is represented in our sampling by a specimen of *Diplodocus* sp., considered an adult based on its femoral length (>150 cm), comparable to individuals with an inferred weight of around 7000 kg (Woodruff *et al.* 2017). The Dicraeosauridae lineage is represented by *Amargasaurus cazaui* Salgado & Bonaparte 1991, a species with mass estimates ranging from 3000 to 10 000 kg, depending on the estimation method used (Benson *et al.* 2014; Bates *et al.* 2015).

Among the Titanosauriformes, the Brachiosauridae *Giraffatitan brancai* Janensch 1914, is sampled as a representative of the upper limit of sauropod body size, with weight estimates reaching up to 30 000 kg (Mazzetta *et al.* 2006; Paul 2019). The Titanosauria, a diverse subgroup within Titanosauriformes, is represented by *Dreadnoughtus schrani* Lacovara *et al.* 2014 and *Uberabatitan ribeiroi* Salgado & Carvalho 2008, both included within the clade Colossosauria (Silva Junior *et al.* 2022), *Australotitan cooperensis* Hocknull *et al.* 2021, which is uncertainly positioned phylogenetically, and *Neuquensaurus australis* Lydekker 1893 (Powell 1992), included within Saltasauridae (Wilson 2002).

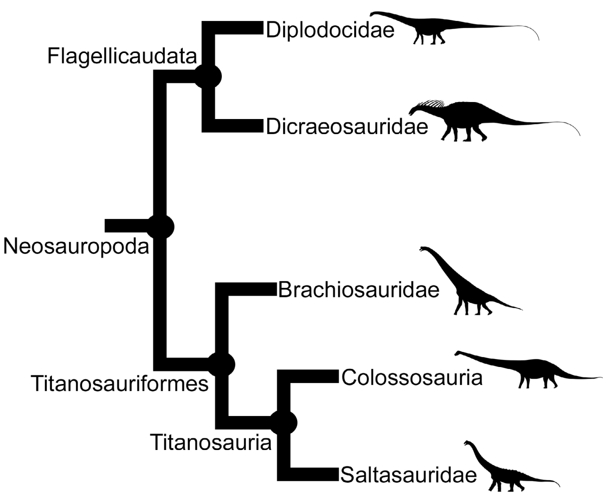

FIG. 1. Simplified phylogenetic relationships of taxa sampled herein (based on Otero & Hutchinson 2022). Silhouettes from PhyloPic (https://www.phylopic.org/). From top to bottom: *Diplodocus carnegii*, *Amargasaurus cazui*, *Cedarosaurus weiskopfae*, *Dreadnoughtus schrani* and *Opisthocoelicaudia skarzynskii*; *D. schrani*, Kenneth Lacovara (CC0 3.0); all others Scott Hartman (CC0 3.0).

Dreadnoughtus, frequently highlighted as one of the largest sauropods, has been attributed a body mass reaching up to 60 000 kg (McPhee *et al.* 2018). However, more conservative estimates suggest a body mass closer to 38 000 kg, comparable to that estimated for *Giraffatitan* (Bates *et al.* 2015). *Australotitan* is also considered to be a large titanosaur. Although no precise body mass estimates are currently available, Hocknull *et al.* (2021) proposed, based on a larger incomplete femur (EMF164), that its body size may have been similar to that of *Dreadnoughtus*.

Neuquensaurus represents the saltasaurid titanosaurs, a group that includes some of the taxa at the lower limit of adult sauropod body size (Navarro *et al.* 2022). Specifically, mass estimates for *Neuquensaurus* range from 1400 to 6000 kg (Benson *et al.* 2014; Bates *et al.* 2015). *Uberabatitan*, though lacking a precise estimated body mass, is represented by its only known complete femur, which is a relatively small element (maximum length of 88 cm) and could suggest a subadult status of this specimen. Larger specimens from its type locality have an estimated length of 26 m (Silva Junior *et al.* 2019), which would place them in a size range comparable to *Dreadnoughtus*.

Institutional abbreviations. CPPLIP, Centro de Pesquisas Paleontológicas Llewellyn Ivor Price, Universidade Federal do Triângulo Mineiro, Uberaba, Brazil; EMF, Eromanga Natural History Museum Fossil, Eromanga, Australia; MACN-Pv, Museo Argentino de Ciencias Naturales 'Bernardino Rivadavia', Coleccíon Nacional Paleontologia de vertebrados, Buenos Aires, Argentina; MB.R., Museum für Naturkunde Berlin, Berlin, Germany; MLP, Museo de La Plata, La Plata, Argentina; MPM, Museo Padre Molina, Río Gallegos, Argentina.

Specimen digitization

The femora of *Amargasaurus cazuai* (MACN-Pv N-15), *Diplodocus sp.* (MACN-Pv 18 814), *Neuquensaurus australis* (MLP 1480), and *Uberabatitan ribeiroi* (CPPLIP-1238) were digitized with a Revopoint® Range handheld scanner, with the meshes created using its proprietary software: Revo Scan 5 (https://global.revopoint3d.com/pages/revoscan5).

The data of the femur of *Australotitan cooperensis* (EMF105) was obtained from MorphoSource (Hocknull & Rochelle 2021), while data of *Dreadnoughtus schrani* (MPM-PV 1156) was obtained from the supplementary material of Lacovara *et al.* (2014). Access to the model of

Giraffatitan brancai (MB.R.5016) was granted by the digital collection of the Museum für Naturkunde, Berlin.

All of the digital specimens were imported as STL-surface models (*.stl) and restored in Blender v4.2.1 (https://www.blender.org/download/). The digital restoration process (Lautenschlager 2016), applied to all femora except for *Giraffatitan* (which required minimal change) corrected cracks and broken surfaces, ensuring the specimens were suitable for biomechanical testing. The meshes were standardized to *c.* 300 000 faces for each model and tested for errors (i.e. non-manifold edges and intersecting faces) using the '3D Print' Blender toolbox. All digitally restored models were uploaded to MorphoSource (Appendix S1) and can be accessed through their respective curators.

Finite element analysis

To simulate *in silico* the loadings experienced by the sauropod femur during the bipedal posture supported by the hindlimb, tests were conducted using FEA (Silva Junior *et al.* 2025). We modelled both extrinsic and intrinsic functional scenarios to test if the femora would be capable of supporting such a posture. The FE models were built using the Blender add-on BFEX (Blender Finite Elements EXporter, Díaz de León-Muñoz *et al.* 2025) to model the different scenarios and solved with Fossils v1.3 using the tangential-plus-normal-traction load model, as it represents the most accurate, life-like model (Chatar *et al.* 2023). The performance of the femora in each test was assessed via mean von Mises stress, considering 98% of the values to avoid individual stress singularities on elements (Figueirido *et al.* 2018; Montefeltro *et al.* 2020).

Based on previous studies that determined that the dinosaur bones are analogous to Haversian bones of fast-growing bovine mammals (Curry 1999; Rayfield *et al.* 2001; Jannel *et al.* 2022), all femora were assigned a Young's modulus (E) value of 10 000 MPa and Poisson's ratio (v) of 0.3.

Extrinsic functional scenarios

Extrinsic tests were modelled for the sauropod femora under bipedal postural scenarios. For this test, all femora were scaled to the same size (1 m), to reduce the effect of the size in our interpretation and to evaluate how the differences only in morphology would impact the stress distribution. To establish stress comparability across models, we applied a normalization process to the compressive load. This normalization used the surface areas of the *Neuquensaurus* femur, accounting for the variation in the number of faces on the meshes within our dataset. We implemented this procedure using the formula introduced by Dumont *et al.* (2009).

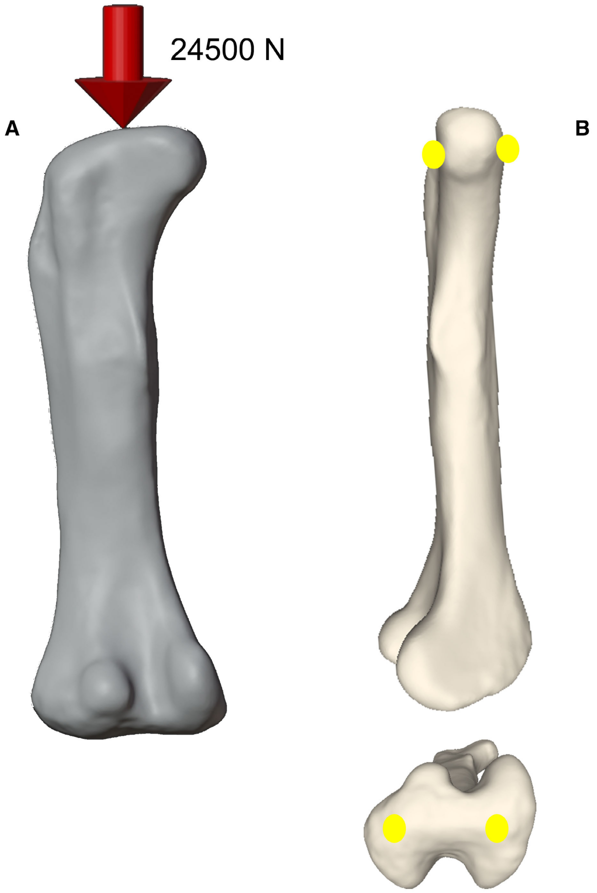

FIG. 2. Extrinsic functional scenario modelled in the study. A, 3D rendering of the femur of *Uberabatitan* (CPPLIP-1238) in posterior view, with the red arrow showing the position of the applied loads. B, representation of the constraints (yellow circles) applied to all models for the extrinsic scenarios.

The loads were applied to a single node at the medial portion of the femoral head (Fig. 2A). A weight of 10 tons was defined as the standard for this functional scenario and the total loads were calculated by multiplying the mass (in kg) by the gravitational acceleration (g = 9.834 m/s^2), resulting in a total load of *c.* 98 000 N. For the functional test, considering that it is unknown whether sauropods used their tail as a third member (thus entering into a tripodal stance) or if the tail was mainly used for support and balance (bipedal stance), with little to no load applied to it, we opted to simulate the total mass distributed only on the hindlimbs (= 49 000 N; i.e. 24 500 N for each femur). Constraints for the extrinsic scenarios were placed on the distal condyles (one on each side), which are aligned with the ground surface, forming a right angle with it, as a means of standardizing the analyses. Two additional constrained nodes at lateral portions of the femoral head, to simulate the femoral articulations to the acetabulum and tibia/fibula. Those nodes were all constrained with zero degrees of freedom (constrained in all axes x, y, and z, Fig. 2B).

Intrinsic functional scenarios

To simulate muscular loads during bipedal posture, we modelled a set of femoral muscles potentially involved in this behaviour. These included *Mm. caudofemoralis longus* and *brevis* (primary femoral retractors contributing to leg rotation and adduction), *Mm. femorotibialis internus* and *externus* (knee extensors), and *adductor femoris* parts I and II (limb stabilizers). Additionally, *M. ischiotrochantericus* (lateral femur rotation) and *M. iliofemoralis* (femur abduction) could act to enhance postural stability. *Mm. extensor* and *flexor digitorum longus* that could help support foot flexion and extension during rearing (*sensu* Gatesy 1990; Otero & Vizcaino 2008; Mallison 2010, 2011; Díez Díaz *et al.* 2020; Voegele *et al.* 2021).

Muscle modelling for each species was based on anatomical correlates, attachment scars on the femora, and previous myological studies (Borsuk-Białynicka 1977; Otero & Vizcaino 2008; Voegele *et al.* 2021). The original scales were used for the femora in these tests to enable accurate calculations of muscle attachment areas for the proposed analysis.

The area of the attachment sites of each muscle (Figs 3A–B, S1) was used as a proxy for the physiological cross-sectional area, which was then multiplied by an isometric muscle stress value of 25.0 N cm^{-2} (Table 1; Porro *et al.* 2011; Montefeltro *et al.* 2020). This approach was selected as it estimates the maximum tension per unit area that each muscle can generate (Thomason 1991), providing a valid scenario for inferring the effort required for rearing. Loads were applied along vectors directed to the respective muscle origins (Fig. 3A–B).

Constraints for the intrinsic scenarios were placed on the distal condyles (one on each side), which are aligned with the ground surface, forming a right angle with it, as a means of standardizing the analysis. This simulates femoral articulations to the tibia/fibula. Those nodes were all constrained with zero degrees of freedom (constrained in all axes x, y, and z, Fig. 3D), allowing an antero-posterior movement of the femoral head.

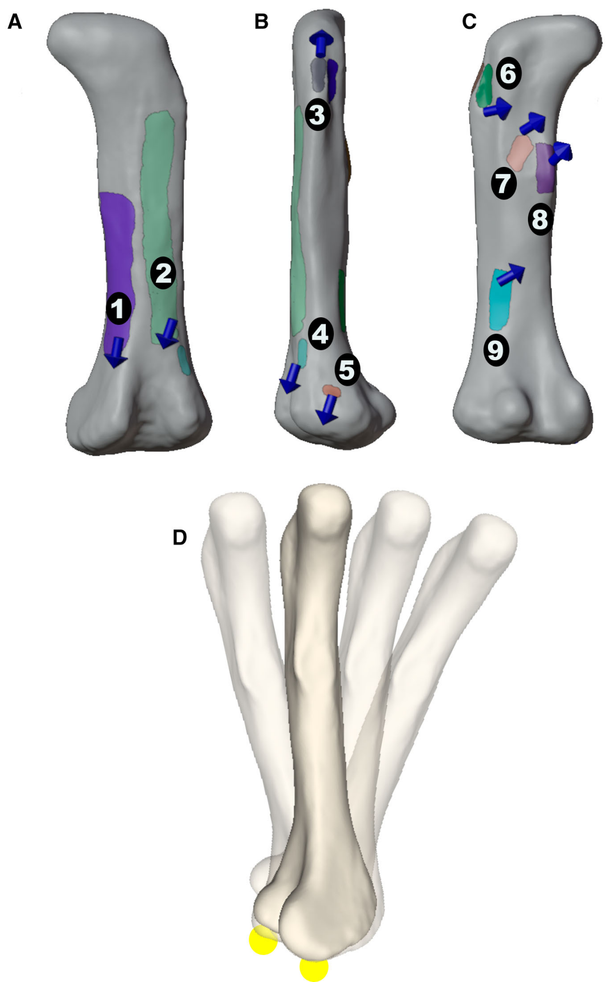

FIG. 3. Intrinsic functional scenario modelled in the study. A–C, 3D renderings of the *Uberabatitan* (CPPLIP-1238) femur (A, anterior; B, lateral; C, posterior view) representing muscular insertions and vectors for load applied. D, representation of the constraints (yellow circles) applied to all models for the intrinsic scenarios, illustrating the movement allowed in the test. *Muscles*: 1, femorotibialis internus; 2, femorotibialis externus; 3, iliofemoralis; 4, extensor digitorum longus; 5, flexor digitorum longus; 6, isquiotrochantericus; 7, adductor femoris I; 8, caudofemoralis longus & caudofemoralis brevis; 9, adductor femoris II.

RESULTS

Extrinsic scenarios

The contour plots of the extrinsic scenarios (Fig. 4) show that the tested sauropod femora reacted similarly in terms of stress distribution across the different species. The most stress-intensive regions are located on the femoral head and the distal third of the femur in all taxa, indicating that stress variation in the tested specimens occurred more in magnitude (mean stress) than in spatial distribution. The mean von Mises stress per element obtained from the tests shows *Neuquensaurus* and *Uberabatitan* with the lowest values during the putative bipedal scenario (1.09 and 1.20 MPa, respectively). In contrast, all other sauropods exceeded a mean value of 1.9 MPa, with *Giraffatitan* showing a stress of 2.51 MPa, nearly twice as high as that of *Neuquensaurus*.

TABLE 1. Total load inferred for each modelled muscle.

Total muscle force (N)	4T	IF	IT	FI	FE	AF1	AF2	EDL	FDL
Amargasaurus	6806	2225	2350	14 673	17 368	3507	3372	1383	653
Australotitan	4843	1490	1847	12 208	16 684	2549	3036	960	550
Diplodocus	2920	1210	1782	9407	16 913	2222	2858	575	326
Dreadnoughtus	8054	3475	8300	20 472	25 802	2516	2878	2450	764
Giraffatitan	9321	3363	7475	19 507	26 862	3780	4103	1617	752
Neuquensaurus	1364	399	622	3247	5309	423	523	292	143
Uberabatitan	2650	463	610	4174	9763	584	603	327	232

Muscle abbreviations: 4T, joint insertion of the *caudofemoralis brevis* and *longus*; AF1, *adductor femoris* I; AF2, *adductor femoris* II; EDL, *extensor digitorum longus*; FDL, *flexor digitorum longus*; FE, *femorotibialis externus*; FI, *femorotibialis internus*; IF, *iliofemoralis*; IT, *ischiotrochantericus*.

Intrinsic scenarios

The results for the intrinsic scenarios show that most of the detected variation in stress among the tested specimens are related to the magnitude instead of the stress distribution along the femora (Fig. 5).

The stress peak is detected in the distal third of the femur across all species, due primarily to the extensive load applied by the *femorotibialis* musculature, which represents the most powerful muscle modelled in our tests (Table 1). The stress is higher on the anterior surface of the shaft, but is also notably high at the medial and lateral surfaces. In posterior view, the region of the fourth trochanter showed reduced stress.

The taxa with the lowest mean stress/elements among the intrinsic scenario (Fig. 5) are *Neuquensaurus* and *Australotitan* (mean of 0.97 and 0.99 MPa, respectively). In contrast, *Uberabatitan* has a mean stress/element of 1.11 MPa, being the fourth most stressed specimen. This pattern is different from the results of the extrinsic scenarios, due to the extensive insertions of the *Mm. femorotibialis* in *Uberabatitan*. The highest value of mean stress/element is measured in *Dreadnoughtus*, with a mean of 15.67 MPa.

DISCUSSION

The plausibility of a bipedal or tripodal stance as a common behaviour among sauropods has been long debated, with various anatomical features suggesting that it may have occurred under specific circumstances. In particular, it has been proposed that saltasaurids were more likely to rear up due to their shorter necks and tails, and overall robust pelvic structure (Powell 1992, 2003). Our results for the saltasaurid *Neuquensaurus* in both scenarios provide further support to this hypothesis, evidencing the combination of a large insertion area for musculature and a robust femur capable of dissipating stress. This suggests that *Neuquensaurus*, and possibly other saltasaurids, may have adopted a bipedal posture more frequently than other sauropods (Wilson & Carrano 1999).

Additionally, Vidal *et al.* (2025) proposed that soft tissue, when associated with pneumatized tails such as those present in *Neuquensaurus* (Cerda *et al.* 2012; Zurriaguz *et al.* 2017), could act as a plastic structure that helps dissipating weight applied to the tail, with the role of pneumatic structures in absorbing loads first demonstrated by Schwarz-Wings *et al.* (2010). This combination of soft tissue and pneumatic adaptations is likely to have reduced stress on the skeletal framework, further supporting the idea that saltasaurids were better equipped to adopt a bipedal stance more frequently or with greater ease than other sauropods.

Previous evidence in favour of a bipedal or tripodal posture in sauropods were based mostly on anatomical traits and only two studies employed a biomechanical or functional approach (Alexander 1985; Mallison 2011). Both studies primarily focused on the centres of mass (COM), arguing that in *Diplodocus*, the COM was located near the hindlimbs, allowing it to rear for extended periods, whereas in *Giraffatitan* (Mallison 2011) the COM was positioned more anteriorly, which would make adopting a bipedal posture more challenging. A similar more anterior COM was also proposed for titanosaurs (Henderson 2006), possibly adding on some resistance to rearing.

Our FEA tests showed that *Giraffatitan* experienced higher stress than *Diplodocus* in both scenarios, although the difference in mean von Mises stress between the two is minimal (Figs 3, 4), thus agreeing with the differences in COM. Overall, these species exhibited the highest stress levels, with the exception of *Dreadnoughtus*. Thus, while *Diplodocus* may have been able to maintain a bipedal stance for longer than *Giraffatitan*, our results provide no evidence to support the notion that this was a frequent behaviour for this taxon, as previously suggested by Mallison (2011). A possible posterior COM can be also

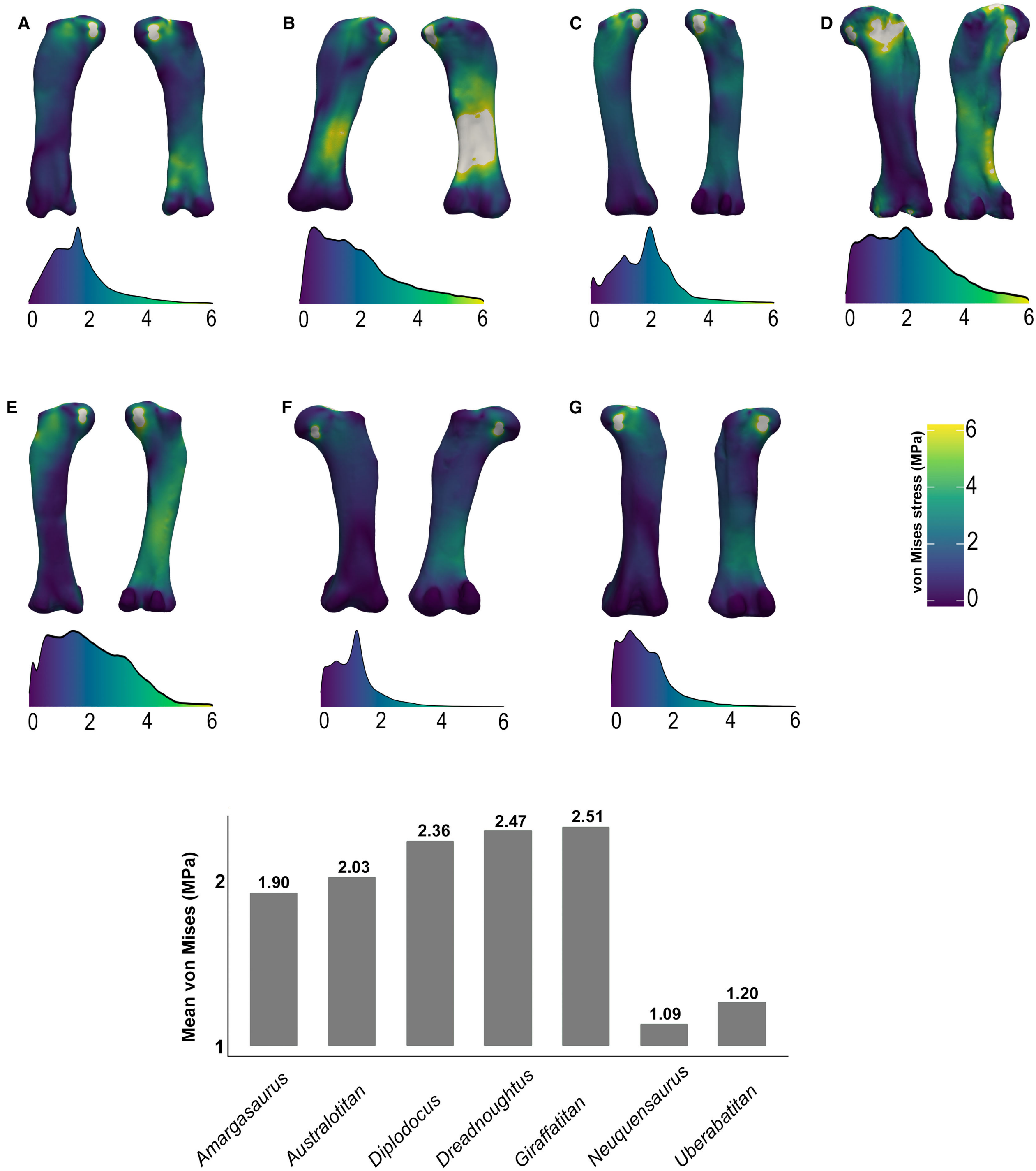

FIG. 4. Von Mises stress contour plots and stress magnitude distributions from finite element analysis of the extrinsic scenarios with an applied load of 24 500 N to sauropod femora in anterior (left) and posterior (right) views of: A, *Amargasaurus*; B, *Australotitan*; C, *Diplodocus*; D, *Dreadnoughtus*; E, *Giraffatitan*; F, *Neuquensaurus* and G, *Uberabatitan*. Regions displayed in white indicate stress value that exceed the upper limit of the defined scale. The mean von Mises stresses are shown below.

inferred for *Amargasaurus*. It was also less stressed than *Diplodocus* in both scenarios, which could indicate a better ability to rear than the former sauropod.

The ability of sauropods to rear up was not only influenced by their centre of mass but also required significant effort from the forelimb musculature, especially for those

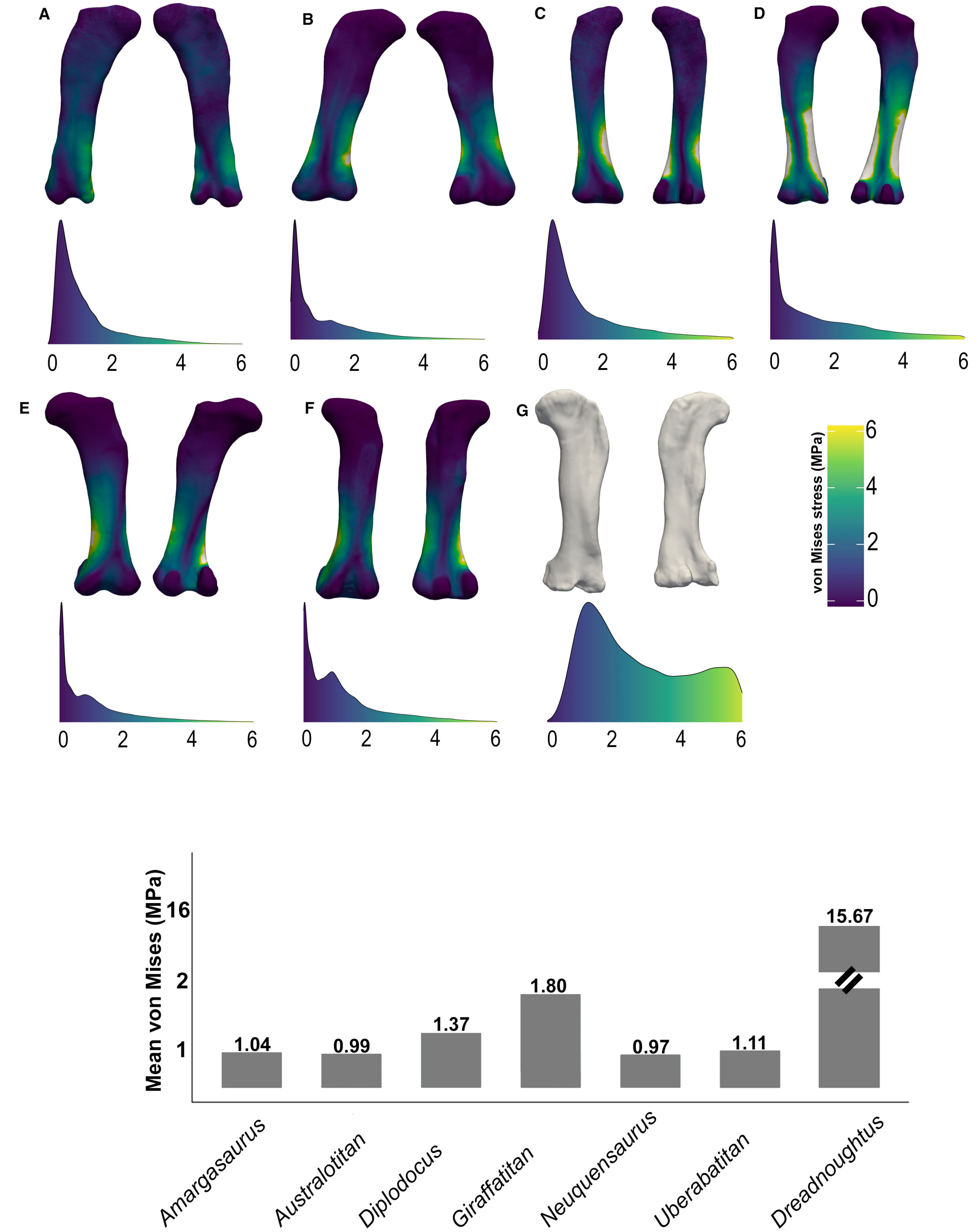

FIG. 5. Von Mises stress contour plots and stress magnitude distributions from finite element analysis of the intrinsic scenarios to sauropod femora in anterior (left) and posterior (right) views of: A, *Amargasaurus*; B, *Australotitan*; C, *Diplodocus*; D, *Giraffatitan*; E, *Neuquensaurus*; F, *Uberabatitan* and G, *Dreadnoughtus*. Regions displayed in white indicate stress value that exceed the upper limit of the defined scale. The mean von Mises stresses are shown below.

taxa with an anteriorly located COM. More comprehensive tests, including the modelling of forelimb musculature, are required to better understand the ability to rear in sauropods.

The mean von Mises stress/element shows differences between the extrinsic and intrinsic scenarios for each modelled taxon. *Uberabatitan* presented the second lowest stress/element in the extrinsic scenarios but was highly stressed during the intrinsic tests. *Australotitan*, on the other hand, shows the lowest stress when the muscle loads were modelled, but yielded near twice the stress/element showed by *Neuquensaurus* in the extrinsic functional model.

One limitation of the FEA tests performed in this study is the absence of modelled cartilaginous tissue, which is known to act as a stress-reducing mechanism, as observed in the pedal pads of sauropods (Jannel *et al.* 2019, 2022). Cartilage can account for up to 10% of bone length (Schwarz *et al.* 2007; Bonnan *et al.* 2010), significantly contributing to stress distribution. Consequently, the stress values reported here are probably overestimated but we prefer to interpret the value as a comparative tool rather than absolute values. As such, given that the elastic properties of cartilage are consistent across vertebrates (Hall 2005; Zhang *et al.* 2009) and that sauropods are likely to have had comparable amounts and distribution of cartilage, the relative stress distribution would remain proportional to the patterns observed in this study. This highlights the influence of femoral shape on stress distribution, as less stressed specimens would still exhibit lower stress levels in a more complex model. This effect is particularly assumed for extrinsic scenarios. In contrast, intrinsic scenarios, in which stress is directly generated by muscles, they would probably be less influenced by the modelling of cartilaginous tissue.

Some later-diverging titanosaurs, such as *Uberabatitan* (Silva Junior *et al.* 2019) and most saltasaurids (i.e. *Rocasaurus* and *Neuquensaurus*; Otero 2010) exhibit a proximodistal scar on the anterior surface of the femora, known as the *linea intermuscularis cranialis* (LIC), which serves as the origin site for the *Mm. femorotibialis internus* and *externus*. This line probably results from increased stress applied by these muscles due to the bevelling of the distal femoral condyles (Voegele *et al.* 2021), creating a condition known as extreme wide-gauge (Wilson & Carrano 1999; Ullmann *et al.* 2017). However, this may represent a secondary change, as the scar is present in early Somphospondyli such as *Diamantinasaurus matildae*, (Poropat *et al.* 2023) and *Garumbatitan morellensis* (Mocho *et al.* 2024).

The LIC significantly increases the surface area for the attachment of the *femorotibialis* musculature which could increase the overall stress created by muscle contraction (Fig. 5). Yet, *Australotitan* and *Neuquensaurus*, in which the LIC is present, exhibited the lowest average of von Mises stress/element in the intrinsic scenario (Fig. 5). In contrast, *Uberabatitan* was one of the most stressed specimens on the intrinsic scenarios (mean of 1.11 MPa), probably due to its wide attachment surface created by the LIC combined with a femur that is less robust than that of *Neuquensaurus* and more mediolaterally compressed than that of *Australotitan*, creating a relatively slender structure.

The extrinsic functional scenario shows that the concentration of weight on the hindlimbs of *Australotitan* highlighted it as one of the most stressed specimens whereas *Uberabatitan* is more capable of enduring the same weight. Hence, just the presence of the LIC, creating a large attachment for the femorotibialis musculature, does not seem to be related to a larger capacity to maintain a bipedal stance.

Dreadnoughtus, a giant titanosaur (Lacovara *et al.* 2014; Gallina *et al.* 2022; Calvo 2023), was the most stressed specimen in the intrinsic and second on the extrinsic scenarios, with almost 5 times the mean von Mises stress of *Neuquensaurus* in the first test and more than 14 times higher than *Giraffatitan* in the second test (Figs 4, 5). The extrinsic scenario results for *Dreadnoughtus* reveal a considerable deviation when compared to other sampled taxa. The muscular reconstruction, following the approach by Voegele *et al.* (2021), does not appear to overestimate the attachment areas when compared to the other models reconstructed here, as such we did not consider it as a factor involved in this result regarding *Dreadnoughtus*. We consider that other aspects of our methodological approach might have been involved in these results.

One of the factors considered is the use of surface models in our analyses. The use of surface models ignores the internal anatomy of the femur and does not consider differences in microanatomy, for example, which is essential in determining bone strength (Augat & Schorlemmer 2006). Sauropod long-limb microanatomy appears to be highly variable: while a thick cortex is found in the dwarf sauropod *Magyarosaurus*, a medullary cavity is observed in the femora of larger species such as *Diplodocus* and *Alamosaurus*, as well as in the dwarf taxa *Europasaurus* (Woodward & Lehman 2009; Mitchell & Sander 2014; Lefebvre *et al.* 2023).

With no information on the three-dimensional microanatomy of *Dreadnoughtus*, there is no way to assess how the ratio of cortical-to-medullary bone could have influenced the material properties of the bones of this specific taxon. However, Lefebvre *et al.* (2023) suggested that microanatomical features were not predominant regarding the weight-bearing function in sauropods. Therefore, the extreme difference found in the results for

Dreadnoughtus is likely to be influenced by its anteroposteriorly compressed femur, combined with the high levels of stress generated by the loads from its own musculature.

Based on our findings, we propose that *Dreadnoughtus* was the least capable of rearing among the taxa studied or, at best, could only sustain this posture for a short duration. This limitation can probably be attributed to its femoral morphology and the significant stress imposed by its own musculature.

Even though our results show that some specimens experienced significantly lower mean von Mises stress/element than others, we also assume that a bipedal or tripodal stance is likely to have been used by all sauropods at least for usual behaviours such as mating, defence, agonistic combat, and foraging. It is also worth noting that sauropods could rely on external support while rearing (such as their mate's body or a tree during feeding) reducing the stress on their hind limbs.

This model represents the first application of FEA to explore the biomechanics of sauropod rearing behaviour and, as such, is subject to methodological limitations that must be acknowledged. The surface-based modelling approach, while computationally efficient and suitable for broad taxonomic comparisons, lacks the detail of internal bone architecture. Although femoral microanatomy varies among sauropods, our models use uniform material properties for all specimens. The exclusion of cartilaginous tissues (key for stress dissipation in living animals) also means that our stress estimates should be seen as comparative, not absolute.

A further limitation that should be considered is the omission of forelimb bones and musculature from our modelling. Supporting and maintaining a bipedal posture would have required coordinated effort from both hind and forelimbs. This is especially relevant for taxa with forward-shifted centres of mass, which may have relied on forelimb strength to counterbalance body weight. Despite those limitations, this study provides the first quantitative, biomechanically informed framework for assessing rearing ability in sauropods. It improves on previous work that relied on qualitative anatomy or simplified mass estimates. The comparative method developed here lays the groundwork for future studies using more detailed models, moving towards a better understanding of sauropod locomotion and behaviour.

Finally, our findings suggest that saltasaurid titanosaurs were the best suited to maintain these postures for extended periods or with greater ease, largely due to their robust femora, which were better equipped to endure the stress. In contrast, giant sauropods, exemplified here by *Dreadnoughtus* and *Giraffatitan*, probably found it more challenging to enter or maintain these postures, as their femora were not robust enough to mitigate the higher loads generated by their massive hindlimb musculature.

CONCLUSION

Our tests, based on mean von Mises stress per element, and stress surface distribution, femoral morphology, and the presence of specific muscular attachments, suggest that some sauropod species could sustain a bipedal stance for extended periods. The results further support the idea that saltasaurid titanosaurs, such as *Neuquensaurus*, may have been better suited for maintaining this posture, potentially aiding these smaller sauropods in reaching food sources. In contrast, *Dreadnoughtus* is the least capable of rearing up or sustaining a bipedal stance for extended periods, probably due to its larger size and particular femoral anatomy. Thus, our findings offer a new perspective on the behavioural ecology of sauropods, emphasizing that morphological adaptations should be considered within a broader context of biomechanical and ecological factors.

Acknowledgements. The authors would like to thank Dr Yanina Herrera for granting access to the La Plata Vertebrate Collection, Dr Scott Hocknull for providing access to the *Australotitan* materials, and Drs Verónica Díez Díaz and Heinrich Mallison for granting access to the digital *Giraffatitan* specimen. We also thank Erick Miguel Díaz de León Muñoz for his assistance with the FEITO BFEX application. Finally, we are grateful to Dr Díez Díaz and the two anonymous reviewers for their comments, which greatly improved the quality of this article. This work was financed by FAPESP (Fundação de Amparo à Pesquisa do Estado de São Paulo; grant to JCGSJ Process Number 2022/14694-3 and 2024/01597-5), and CNPq (Conselho Nacional de Desenvolvimento Científico e Tecnológico; grant to FCM and TSM). The Article Processing Charge for the publication of this research was funded by the Coordenação de Aperfeiçoamento de Pessoal de Nível Superior - Brasil (CAPES) (ROR identifier: 00x0ma614).

Author contributions. **Conceptualization** Julian Silva Junior (JSJ), Felipe Montefeltro (FM), Gabriel Ferreira (GSF); **Data Curation** JSJ, Thiago Marinho (TM), Agustín Martinelli (AM); **Formal Analysis** JSJ, FM, GSF; **Funding acquisition** JSJ; **Investigation** JSJ, FM, GSF, TM, AM; **Methodology** JSJ, FM, GSF; **Project administration** JSJ, FM; **Visualization** JSJ, FM, GSF; **Writing – Original Draft Preparation** JSJ, FM, GSF; **Writing – Review & Editing** JSJ, FM, GSF, TM, AM.

DATA ARCHIVING STATEMENT

Data for this study (including stress results and scripts used for analyses) are available in the Dryad digital repository: https://doi.org/10.5061/dryad.2ngf1vj00.

Editor. Philip Mannion

SUPPORTING INFORMATION

Additional Supporting Information can be found online (https://doi.org/10.1111/pala.70019):

Figure S1. Musculature reconstructed to the intrinsic models (*.tiff). Meshes retrieved from Blender with random colours attributed. Elements not to scale.

Appendix S1. MorphoSource DOIs for specimens scanned for this study.

REFERENCES

Alexander, R. M. 1985. Mechanics of posture and gait of some large dinosaurs. *Zoological Journal of the Linnean society*, **83** (1), 1–25.

Augat, P. and Schorlemmer, S. 2006. The role of cortical bone and its microstructure in bone strength. *Age and ageing*, **35** (suppl_2), ii27–ii31.

Bakker, R. T. 1978. Dinosaur feeding behavior and the origin of flowering plants. *Nature*, **274** (5672), 661–663.

Bakker, R. T. 1986. *The dinosaur heresies: New theories unlocking the mystery of the dinosaurs and their extinction*. William Morrow.

Bates, K. T., Falkingham, P. L., Macaulay, S., Brassey, C. and Maidment, S. C. 2015. Downsizing a giant: re-evaluating *Dreadnoughtus* body mass. *Biology Letters*, **11** (6), 20150215.

Benson, R. B., Campione, N. E., Carrano, M. T., Mannion, P. D., Sullivan, C., Upchurch, P. and Evans, D. C. 2014. Rates of dinosaur body mass evolution indicate 170 million years of sustained ecological innovation on the avian stem lineage. *PLoS Biology*, **12** (5), e1001853.

Bonnan, M. F., Sandrik, J. L., Nishiwaki, T., Wilhite, D. R., Elsey, R. M. and Vittore, C. 2010. Calcified cartilage shape in archosaur long bones reflects overlying joint shape in stress-bearing elements: implications for nonavian dinosaur locomotion. *The Anatomical Record*, **293** (12), 2044–2055.

Borsuk-Białynicka, M. 1977. A new camarasaurid sauropod *Opisthocoelicaudia skarzynskii* gen. n., sp. n. from the Upper Cretaceous of Mongolia. *Palaeontologia Polonica*, **37** (5), 5–64.

Calvo, J. O. 2023. What is the most giant sauropod from Argentina? Diversity of large titanosaurs from Patagonia. *Metode Science Studies Journal*, **14**, 65–75.

Carballido, L., Pol, D., Otero, A., Cerda, I. A., Salgado, L., Garrido, A. C., Ramezani, J., Cúneo, N. R. and Krause, J. M. 2017. A new giant titanosaur sheds light on body mass evolution among sauropod dinosaurs. *Proceedings of the Royal Society B*, **284**, 20171219.

Cerda, I. A., Salgado, L. and Powell, J. E. 2012. Extreme postcranial pneumaticity in sauropod dinosaurs from South America. *Paläontologische Zeitschrift*, **86**, 441–449.

Chatar, N., Boman, R., Fallon Gaudichon, V., Maclaren, J. A. and Fischer, V. 2023. 'Fossils': a new, fast and open-source protocol to simulate muscle-driven biomechanical loading of bone. *Methods in Ecology and Evolution*, **14** (3), 848–859.

Cunningham, J. A., Rahman, I. A., Lautenschlager, S., Rayfield, E. J. and Donoghue, P. C. 2014. A virtual world of paleontology. *Trends in Ecology and Evolution*, **29** (6), 347–357.

Curry, K. A. 1999. Ontogenetic histology of *Apatosaurus* (Dinosauria: Sauropoda): new insights on growth rates and longevity. *Journal of Vertebrate Paleontology*, **19** (4), 654–665.

Díaz de León-Muñoz, E. M., Boman, R. and Ferreira, G. S. 2025. BFEX: a toolbox for finite element analysis with fossils and blender. *Ecology and Evolution*, **15** (3), e71093.

Díez Díaz, V., Demuth, O. E., Schwarz, D. and Mallison, H. 2020. The tail of the Late Jurassic sauropod *Giraffatitan brancai*: digital reconstruction of its epaxial and hypaxial musculature, and implications for tail biomechanics. *Frontiers in Earth Science*, **8**, 160.

Dodson, P. 1990. Sauropoda. 345–401. *In* Weishampel, D. B., Dodson, P. and Osmolska, H. (eds) *The Dinosauria*, First edition. University of California Press.

Dumont, E. R., Grosse, I. R. and Slater, G. J. 2009. Requirements for comparing the performance of finite element models of biological structures. *Journal of Theoretical Biology*, **256** (1), 96–103.

Falkingham, P. L., Margetts, L. and Manning, P. L. 2010. Fossil vertebrate tracks as paleopenetrometers: confounding effects of foot morphology. *PALAIOS*, **25** (6), 356–360.

Figueirido, B., Lautenschlager, S., Pérez-Ramos, A. and Van Valkenburgh, B. 2018. Distinct predatory behaviors in scimitar-and dirk-toothed sabertooth cats. *Current Biology*, **28** (20), 3260–3266.

Gallina, P. A., González Riga, B. J. and Ortiz David, L. D. 2022. Time for giants: titanosaurs from the Berriasian–Santonian age. 299–340. *In* Otero, A., Carballido, J. L. and Pol, D. (eds) *South American sauropodomorph dinosaurs: Record, diversity and evolution*. Springer.

Gatesy, S. M. 1990. Caudofemoral musculature and the evolution of theropod locomotion. *Paleobiology*, **16** (2), 170–186.

Hall, B. K. 2005. *Bones and cartilage: Developmental and evolutionary skeletal biology*. Elsevier.

Hatcher, J. B. 1901. *Diplodocus* (Marsh): its osteology, taxonomy, and probable habits, with a restoration of the skeleton. *Memoirs of the Carnegie Museum*, **1**, 1–63.

Henderson, D. M. 2006. Burly gaits: centers of mass, stability, and the trackways of sauropod dinosaurs. *Journal of Vertebrate Paleontology*, **26** (4), 907–921.

Hocknull, S. and Rochelle, L. 2021. A new giant sauropod, *Australotitan cooperensis* gen. et sp. nov., from the mid-Cretaceous of Australia. [Dataset] MorphoSource. https://www.morphosource.org/concern/biological_specimens/000359486

Hocknull, S. A., Wilkinson, M., Lawrence, R. A., Konstantinov, V., Mackenzie, S. and Mackenzie, R. 2021. A new giant sauropod, *Australotitan cooperensis* gen. et sp. nov., from the mid-Cretaceous of Australia. *PeerJ*, **9**, e11317.

Janensch, W. 1914. Übersicht über die Wirbeltierfauna der Tendaguruschichten, nebst einer kurzer Charakterisierung der neu aufgeführten Arten von Sauropoden. *Archiv für Biontologie*, **3**, 81–110.

Jannel, A., Nair, J. P., Panagiotopoulou, O., Romilio, A. and Salisbury, S. W. 2019. "Keep your feet on the ground": simulated range of motion and hind foot posture of the Middle Jurassic sauropod *Rhoetosaurus brownei* and its implications for sauropod biology. *Journal of Morphology*, **280** (6), 849–878.

Jannel, A., Salisbury, S. W. and Panagiotopoulou, O. 2022. Softening the steps to gigantism in sauropod dinosaurs through the evolution of a pedal pad. *Science Advances*, **8** (31), eabm8280.

Klinkhamer, A. J., Mallison, H., Poropat, S. F., Sloan, T. and Wroe, S. 2018. Comparative three-dimensional moment arm analysis of the sauropod forelimb: implications for the transition to a wide-gauge stance in titanosaurs. *The Anatomical Record*, **302** (5), 794–817.

Lacovara, K. J., Lamanna, M. C., Ibiricu, L. M., Poole, J. C., Schroeter, E. R., Ullmann, P. V. and Novas, F. E. 2014. A gigantic, exceptionally complete titanosaurian sauropod dinosaur from southern Patagonia, Argentina. *Scientific Reports*, **4** (1), 6196.

Lautenschlager, S. 2016. Reconstructing the past: methods and techniques for the digital restoration of fossils. *Royal Society Open Science*, **3** (10), 160342.

Lefebvre, R., Houssaye, A., Mallison, H., Cornette, R. and Allain, R. 2022. A path to gigantism: three-dimensional study of the sauropodomorph limb long bone shape variation in the context of the emergence of the sauropod bauplan. *Journal of Anatomy*, **241** (2), 297–336.

Lefebvre, R., Allain, R. and Houssaye, A. 2023. What's inside a sauropod limb? First three-dimensional investigation of the limb long bone microanatomy of a sauropod dinosaur, *Nigersaurus taqueti* (Neosauropoda, Rebbachisauridae), and implications for the weight-bearing function. *Palaeontology*, **66** (4), e12670.

Lydekker, R. 1893. The dinosaurs of Patagonia. *Anales Museo de La Plata*, **2**, 1–14.

Mallison, H. 2010. The digital *Plateosaurus* I: body mass, mass distribution, and posture assessed using CAD and CAE on a digitally mounted complete skeleton. *Palaeontologia Electronica*, **13** (2), 8A.

Mallison, H. 2011. Rearing giants: kinetic-dynamic modeling of sauropod bipedal and tripodal poses. 237–250. *In* Klein, N., Remes, K., Gee, C. T. and Sander, P. M. (eds) *Biology of the sauropod dinosaurs: Understanding the life of giants*. Indiana University Press.

Mazzetta, G. V., Christiansen, P. and Fariña, R. A. 2006. Giants and bizarres: body size of some southern South American Cretaceous dinosaurs. *Historical Biology*, **16** (2-4), 71–83.

McPhee, B. W., Benson, R. B., Botha-Brink, J., Bordy, E. M. and Choiniere, J. N. 2018. A giant dinosaur from the earliest Jurassic of South Africa and the transition to quadrupedality in early sauropodomorphs. *Current Biology*, **28** (19), 3143–3151.

Mitchell, J. and Sander, P. M. 2014. The three-front model: a developmental explanation of long bone diaphyseal histology of Sauropoda. *Biological Journal of the Linnean Society*, **112** (4), 765–781.

Mocho, P., Escaso, F., Gasulla, J. M., Galobart, À., Poza, B., Santos-Cubedo, A. and Ortega, F. 2024. New sauropod dinosaur from the Lower Cretaceous of Morella (Spain) provides new insights on the evolutionary history of Iberian somphospondylan titanosauriforms. *Zoological Journal of the Linnean Society*, **201** (1), 214–268.

Montefeltro, F. C., Lautenschlager, S., Godoy, P. L., Ferreira, G. S. and Butler, R. J. 2020. A unique predator in a unique ecosystem: modelling the apex predator within a Late Cretaceous crocodyliform-dominated fauna from Brazil. *Journal of Anatomy*, **237** (2), 323–333.

Navarro, B. A., Ghilardi, A. M., Aureliano, T., Díez Díaz, V., Bandeira, K. L., Cattaruzzi, A. G. and Zaher, H. 2022. A new nanoid titanosaur (Dinosauria: Sauropoda) from the Upper Cretaceous of Brazil. *Ameghiniana*, **59** (5), 317–354.

Otero, A. 2010. The appendicular skeleton of *Neuquensaurus*, a Late Cretaceous saltasaurine sauropod from Patagonia, Argentina. *Acta Palaeontologica Polonica*, **55** (3), 399–426.

Otero, A. and Hutchinson, J. R. 2022. Body size evolution and locomotion in Sauropodomorpha: what the South American record tells us. 443–472. *In* Otero, A., Carballido, J. L. and Pol, D. (eds) *South American sauropodomorph dinosaurs*. Springer.

Otero, A. and Vizcaino, S. F. 2008. Hindlimb musculature and function of *Neuquensaurus australis* (Sauropoda: Titanosauria). *Ameghiniana*, **45** (2), 333–348.

Paul, G. S. 2019. Determining the largest known land animal: a critical comparison of differing methods for restoring the volume and mass of extinct animals. *Annals of the Carnegie Museum*, **85** (4), 335–358.

Poropat, S. F., Mannion, P. D., Rigby, S. L., Duncan, R. J., Pentland, A. H., Bevitt, J. J. and Elliott, D. A. 2023. A nearly complete skull of the sauropod dinosaur *Diamantinasaurus matildae* from the Upper Cretaceous Winton Formation of Australia and implications for the early evolution of titanosaurs. *Royal Society Open Science*, **10** (4), 221618.

Porro, L. B., Holliday, C. M., Anapol, F., Ontiveros, L. C., Ontiveros, L. T. and Ross, C. F. 2011. Free body analysis, beam mechanics, and finite element modeling of the mandible of *Alligator mississippiensis*. *Journal of Morphology*, **272** (8), 910–937.

Powell, J. E. 1992. Osteología de *Saltasaurus loricatus* (Sauropoda – Titanosauridae) del Cretácico Superior del noroeste Argentino. 165–230. *In* Sanz, J. L. and Buscalioni, A. D. (eds) *Los dinosaurios y su entorno biotico*. Institutio Juan de Valdes. Actas del Segundo Curso de Paleontologia in Cuenca.

Powell, J. E. 2003. Revision of South American titanosaurid dinosaurs: palaeobiological, palaeobiogeographical and phylogenetic aspects. *Records of the Queen Victoria Museum Launceston*, **111**, 1–173.

Rayfield, E. J. 2007. Finite element analysis and understanding the biomechanics and evolution of living and fossil organisms. *Annual Review of Earth and Planetary Sciences*, **35** (1), 541–576.

Rayfield, E. J., Norman, D. B., Horner, C. C., Horner, J. R., Smith, P. M., Thomason, J. J. and Upchurch, P. 2001. Cranial design and function in a large theropod dinosaur. *Nature*, **409** (6823), 1033–1037.

Rowe, A. J. and Rayfield, E. J. 2022. The efficacy of computed tomography scanning versus surface scanning in 3D finite element analysis. *PeerJ*, **10**, e13760.

Salgado, L. and Bonaparte, J. F. 1991. A new dicraeosaurid sauropod, *Amargasaurus cazaui* gen. et. sp. nov., from the La Amarga Formation, Neocomian of Neuquén Province, Argentina. *Ameghiniana*, **28**, 333–346.

Salgado, L. and Carvalho, I. S. 2008. *Uberabatitan ribeiroi*, a new titanosaur from the Marília formation (Bauru group, Upper Cretaceous), Minas Gerais, Brazil. *Palaeontology*, **51** (4), 881–901.

Sander, P. M., Christian, A., Clauss, M., Fechner, R., Gee, C. T., Griebeler, E. M. and Witzel, U. 2011. Biology of the sauropod dinosaurs: the evolution of gigantism. *Biological Reviews*, **86** (1), 117–155.

Schwarz, D., Wings, O. and Meyer, C. A. 2007. Super sizing the giants: first cartilage preservation at a sauropod dinosaur limb joint. *Journal of the Geological Society*, **164** (1), 61–65.

Schwarz-Wings, D., Meyer, C. A., Frey, E., Manz-Steiner, H. R. and Schumacher, R. 2010. Mechanical implications of pneumatic neck vertebrae in sauropod dinosaurs. *Proceedings of the Royal Society B*, **277** (1678), 11–17.

Silva Junior, J. C. G., Marinho, T. S., Martinelli, A. G. and Langer, M. C. 2019. Osteology and systematics of *Uberabatitan ribeiroi* (Dinosauria; Sauropoda): a Late Cretaceous titanosaur from Minas Gerais, Brazil. *Zootaxa*, **4577** (3), 401–438.

Silva Junior, J. C. G., Montefeltro, F. C., Marinho, T. S., Martinelli, A. G. and Langer, M. C. 2021. Finite elements analysis suggests a defensive role for osteoderms in titanosaur dinosaurs (Sauropoda). *Cretaceous Research*, **129**, 105031.

Silva Junior, J. C., Martinelli, A. G., Iori, F. V., Marinho, T. S., Hechenleitner, E. M. and Langer, M. C. 2022. Reassessment of *Aeolosaurus maximus*, a titanosaur dinosaur from the Late Cretaceous of southeastern Brazil. *Historical Biology*, **34** (3), 403–411.

Silva Junior, J. C. G., Ferreira, G. S., Martinelli, A. G., Marinho, T. S. and Montefeltro, F. C. 2025. Data from: Standing giants: a digital biomechanical model for bipedal postures in Sauropod Dinosaurs [Dataset]. Dryad. https://doi.org/10.5061/dryad.2ngf1vj00

Taylor, M. P., Hone, D. W., Wedel, M. J. and Naish, D. 2011. The long necks of sauropods did not evolve primarily through sexual selection. *Journal of Zoology*, **285** (2), 150–161.

Thomason, J. J. 1991. Cranial strength in relation to estimated biting forces in some mammals. *Canadian Journal of Zoology*, **69** (9), 2326–2333.

Ullmann, P. V., Bonnan, M. F. and Lacovara, K. J. 2017. Characterizing the evolution of wide-gauge features in stylopodial limb elements of titanosauriform sauropods via geometric morphometrics. *The Anatomical Record*, **300** (9), 1618–1635.

Upchurch, P., Barrett, P. M. and Dodson, P. 2004. Sauropoda. 259–322. *In The Dinosauria*, Second edition. University of California Press.

Vidal, D., Mocho, P., Aberasturi, A., Sanz, J. L. and Ortega, F. 2020. High browsing skeletal adaptations in *Spinophorosaurus* reveal an evolutionary innovation in sauropod dinosaurs. *Scientific Reports*, **10** (1), 6638.

Vidal, L. S., Bergqvist, L. P., Candeiro, C. R., Bandeira, K. L., Tavares, S., Ribeiro, T. B. and Pereira, P. V. 2025. Biomechanics and morphological comparisons of the caudal region of titanosaurs from the Cretaceous of Brazil: paleobiology and paleoecology inferences. *Journal of Anatomy*, **246** (1), 20–44.

Voegele, K. K., Ullmann, P. V., Lamanna, M. C. and Lacovara, K. J. 2021. Myological reconstruction of the pelvic girdle and hind limb of the giant titanosaurian sauropod dinosaur *Dreadnoughtus schrani*. *Journal of Anatomy*, **238** (3), 576–597.

Whitlock, J. A. 2011. A phylogenetic analysis of Diplodocoidea (Saurischia: Sauropoda). *Zoological Journal of the Linnean Society*, **161** (4), 872–915.

Wilson, J. 2002. Sauropod dinosaur phylogeny: critique and cladistic analysis. *Zoological Journal of the Linnean Society*, **136** (2), 215–275.

Wilson, J. A. and Carrano, M. T. 1999. Titanosaurs and the origin of "wide-gauge" trackways: a biomechanical and systematic perspective on sauropod locomotion. *Paleobiology*, **25** (2), 252–267.

Woodruff, D. C., Fowler, D. W. and Horner, J. R. 2017. A new multi-faceted framework for deciphering diplodocid ontogeny. *Palaeontologia Electronica*, **20** (3), 43A.

Woodward, H. N. and Lehman, T. M. 2009. Bone histology and microanatomy of *Alamosaurus sanjuanensis* (Sauropoda: Titanosauria) from the maastrichtian of Big Bend National Park, Texas. *Journal of Vertebrate Paleontology*, **29** (3), 807–821.

Zhang, G., Eames, B. F. and Cohn, M. J. 2009. Evolution of vertebrate cartilage development. *Current Topics in Developmental Biology*, **86**, 15–42.

Zurriaguz, V., Martinelli, A., Rougier, G. W. and Ezcurra, M. D. 2017. A saltasaurine titanosaur (Sauropoda: Titanosauriformes) from the Angostura Colorada Formation (upper Campanian, Cretaceous) of northwestern Patagonia, Argentina. *Cretaceous Research*, **75**, 101–114.